

# DIVIDE AND PREDICT: AN ARCHITECTURE FOR INPUT SPACE PARTITIONING AND ENHANCED ACCURACY

FENIX W. HUANG, HENNING S. MORTVEIT, AND CHRISTIAN M. REIDYS

**ABSTRACT.** In this article the authors develop an intrinsic measure for quantifying heterogeneity in training data for supervised learning. This measure is the variance of a random variable which factors through the influences of pairs of training points. The variance is shown to capture data heterogeneity and can thus be used to assess if a sample is a mixture of distributions. The authors prove that the data itself contains key information that supports a partitioning into blocks. Several proof of concept studies are provided that quantify the connection between variance and heterogeneity for EMNIST image data and synthetic data. The authors establish that variance is maximal for equal mixes of distributions, and detail how variance-based data purification followed by conventional training over blocks can lead to significant increases in test accuracy.

## 1. INTRODUCTION

The pursuit of advances in machine learning and generative AI has led to a massive increase in computing requirements. Complex data containing multiple distributions has led to more data-hungry and advanced architectures, running on increasingly larger data centers with power demands equivalent to those of mid-size cities, have definitely led to breakthroughs. What about advances in the underlying theory?

This paper introduces a novel measure that captures *heterogeneity* of mixed distributions. The measure offers an intrinsic way to quantify data complexity. Furthermore, we prove that there exists an algorithm that allows one to “untangle” the data. Our theory thus supports untangling data which in turn enables the use of simpler architectures that maintain high accuracy, but have a significantly smaller energy footprint.

Our measure is based on the notion of influence introduced in the 1980s (see, e.g., [7]) and was motivated by the high cost of model retraining. Influence is genuinely local in the sense that it is associated with specific pairs of data points and was used to quantify how model parameters for local loss contributions change as we perturb a training point by an infinitesimal amount. This led to a data-calculus, capable of deriving closed form expressions of training data perturbations. The topic was revisited in [16] in the context of machine learning, where the authors showed how influence can be used to expose vulnerability of training data, as well as how to easily manipulate training data to force counterintuitive results, making the case that influence functions represent a useful instrument to understand black-box predictions. However, robust statistics shows that when the influence function is unbounded, even an infinitesimal perturbation of the data can induce arbitrarily large changes in the estimator, particularly when the assumed model fails to adequately represent the observed data distribution [12].

The key contribution of this paper is to treat influence as a global measure of a data set instead of as a local measure at pairs of data points, and to demonstrate the feasibility of

---

*Key words and phrases.* Supervised learning, training data stratification, influence, heterogeneity.

using this concept to partition training data into blocks on which existing machine learning methods exhibit higher test accuracy.

Supervised learning takes a set of the form

$$(1) \quad Z = \{z_i = (x_i, y_i) \mid x_i \in E, y_i \in \mathbb{R} \text{ for } 1 \leq i \leq n\},$$

where  $E$  is some suitable space (e.g., images or  $\mathbb{R}^k$ ), a parametrized model class  $\mathcal{F}_\theta$  with  $\theta \in \mathbb{R}^m$ , a real-valued *loss function*  $\mathcal{L}_Z$ , and seeks to determine

$$(2) \quad \hat{\theta} = \arg \min_{\theta} \mathcal{L}_Z(F_\theta),$$

where the primary objective is a model with high prediction quality. There are now a range of advanced, computationally demanding architectures to tackle this problem. Examples include deep neural networks [18], Mixture of Experts [22], and, more recently, transformers with self-attention mechanisms [28, 20, 10]. A common assumption is that the *training set*  $Z$  is a sample from some input-output process that can be captured well by a single statistical distribution  $p(y|x, \hat{\theta})$ . However, even advanced models can struggle when this is not the case.

As for quality of prediction, the convergence framework of sufficiently over-parameterized networks [1] guarantees close to zero training loss for any non-degenerate data set at a global minimum. When generalization falls short of expectations, a common strategy is to employ more complex models or architectures. However, recent studies on learning from heterogeneous or mixture data indicate that a single global model fails to recover the individual components, and merely increasing model capacity does not resolve the errors induced by such heterogeneity [14, 21, 27]. Alternatively, various extrinsic measures, such as the use of domain experts, may be employed to organize data or remove “outliers”. A Variational Autoencoder (VAE) is a framework that maps inputs into a latent space, enabling effective representation learning, dimensionality reduction, and modeling of complex data distributions [15]. However, standard VAE assumes a unimodal latent prior and therefore cannot reliably separate distinct mixtures of distributions in the data. When the latent representations of different sub-populations overlap, the decoder will produce outputs biased toward a global average rather than capturing each distribution individually [17, 26].

The notion of *mixture models* emerged in the statistical literature to address the situation where this assumption fails. This work is largely concerned with the case where  $Z$  arises through  $K$  (a hyperparameter) identical distributions (e.g., Gaussians) albeit with different parameters. The work has been extended to mixtures of non-identical distributions, see [23].

A *mixture of experts* (MoE) is a machine learning architecture with multiple specialized sub-models referred to as *experts* and a gating network routing input to the subset of the sub-models. It was introduced in [8, 22, 5, 25, 2] based on the fundamental assumption that the input features contain sufficient signal to allow the gating network (router) to distinguish between the underlying distributions. The presence of such a signal is essential [14, 13]: suppose we have data generated by two different functions and no further information. Then the MoE encounters a one-to-many mapping problem and the router has no basis to partition the data. As a result, gating weights converge towards an equal distribution. That is, the model will minimize the global loss by predicting an average function, rather than recovering the individual functions, a shortcoming induced by the heterogeneity in the latent labels rather than the observed features.

Our approach is motivated by prior work on multiple sequence arrays of viral RNA sequences [3]. Here data-heterogeneity manifests through a mixture of viral variants in the

data, and the objective is to partition the data into these variants. Such determinations are typically accomplished with the help of experts and experiments. In [3] a different method is introduced which is based on studying the change of the variance of information between two columns of the array. It is shown that there always exist sequences whose removal lower the variance of information leading to a procedure by which blocks of sequences belonging to a single variant can be identified. The key here is that a variant corresponds to a set of molecular bonds (motif) which in turn relates certain columns. Lowering the variance of information is then achieved by removing sequences that are not consistent with these relations. In the context of machine learning, choices of loss functions and architectures can be seen as proxies for these motives. It is therefore natural to consider utilizing the data-removal induced change of information fabric to identify sub-samples of data that are “homogeneous”.

Let  $Z$  represent a mix of distributions without making assumptions about their nature or numbers. The results of this paper suggest considering a two-stage approach to supervised learning: a stratification step where  $Z$  is partitioned into sets  $Z_1$  through  $Z_k$ , followed by a training step for individual sub-models over the various  $Z_i$ ’s. Subsequent prediction uses a classifier to route input to the appropriate sub-model which is then applied, see Figure 1.

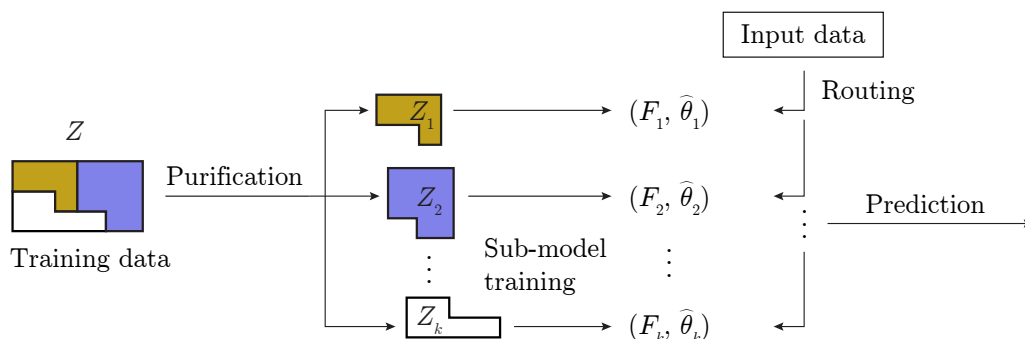


FIGURE 1. The two-stage approach involving purification followed by conventional machine learning. Prediction is done using a classifier routing input to the appropriate sub-model.

To describe our approach we fix a model class  $\mathcal{F}_\theta$ , loss function  $f_Z(\theta) = \sum_z L(z, \theta)$ , and introduce the augmented function  $u_Z(\theta) = f_Z(\theta) + \sum_z \epsilon_z L(z, \theta)$ . In [16], using the framework of [7], it is shown that for  $z, z' \in Z$ , the derivative  $\frac{\partial}{\partial \epsilon_z} L(z', \theta)$  quantifies the influence of the scaling of  $z$  on the loss at  $z'$ , and that this derivative can be positive as well as negative, even when  $Z$  consists of a single distribution.

To extend local influence to a global concept of data set influence, we introduce a random variable  $X$  defined over pairs  $\{z, z'\} \subset Z$  by  $X(\{z, z'\}) = \left[ \frac{\partial}{\partial \epsilon_z} L(z', \hat{\theta}) \right]$ . The properties of  $X$  encapsulate features of the entire data set. Clearly,  $X$  depends on the model class, loss function as well as the model  $\hat{\theta}$ . Once global data properties are framed as a random variable, a natural next step is to consider its moments  $\mathbb{E}[X^\ell]$ . Intuitively, the variance should be minimized to obtain blocks  $Z_i$  following a single distribution. In order to stratify the set  $Z$  into blocks of minimal variance the key question is therefore if we can iteratively remove subsets  $M$  to minimize the variance, thereby breaking up  $Z$  into “homogeneous” pieces.

Our main results are Theorems 1 and 2 which, under mild assumptions on the size of  $Z$ , but also convexity, guarantee the existence of a set  $M$  whose removal lowers the variance as well as the even-ordered raw moments of  $X$ . The implication of these results is that stratification of  $Z$  and subsequent training of sub-models can increase test accuracy relative to the direct approach of conventional training on  $Z$ . Our proof-of-concept experiments indicate that the increase in test accuracy can be quite significant, even when the convexity assumption fails to hold.

We emphasize that the blocks generated through the stratification depend on the underlying loss function and model class  $\mathcal{F}_\theta$ . Stratification mimics what happens in experimental physics where parameters and methods are set and specific answers are derived accordingly. The choice of model class and loss function are tantamount to the choice of experimental setup. We remark that the stratification itself constitutes a window into the “black box” of the learning process itself. Here, using a sufficiently expressive model (which exist by [1]) to probe  $Z$  through moments and variance allows one to identify the presence of multiple distributions within the input data.

Suppose the data follows a single, unique distribution and that we have a model,  $\hat{\theta}$ , with a sufficiently small loss. In this scenario the influence for any pair  $z \neq z'$  is arguably minimal, i.e.,  $\frac{\partial}{\partial \epsilon_z} L(z', \theta)$  has a small absolute value and fluctuations are induced by the varying closeness of the particular  $z, z'$  to the model. In case the input data contains multiple distributions two effects manifest: first the quality of the model in terms of prediction can only decrease, and secondly the absolute values of the derivatives become larger and larger—even though the loss function is still small as guaranteed by [1]. It is informative to consider the first effect taken to its extreme, namely an input data set that is entirely random. In this scenario influence measurements are of limited value since they are relative to the loss function and network employed. Random data hinders any inferences obtained from employing these.

The paper is organized as follows: In Section 2 we establish terminology and some basic facts (Lemma 1 through 3) for how to express influence via the Hessian [16, 7]. In Section 3 we cover Theorem 1, Theorem 2, and Corollary 1 which, under the assumption of convexity, establish the fact that there are data points whose removal will reduce the variance of  $X$ . A proof outline is provided for Theorem 1; the full proof is given in Section 6 along with proofs of all supporting results. Section 4 provides proof-of-concept applications showing how variance captures heterogeneity and how variance-based purification outlined in Figure 1 can lead to a large increase in test accuracy. Results are established for EMNIST image data and synthetic data. The discussion in Section 5 includes an entropy perspective on the heterogeneity captured by the random variable  $X$  as well as an outlook.

## 2. SOME PRELIMINARY FACTS

In the following, we will suppress the model class  $\mathcal{F}$  thus identifying  $F_\theta$  with  $\theta$ , and, by common convention, will consider loss functions of the form

$$(3) \quad f_Z(\theta) = \frac{1}{n} \sum_{z \in Z} L(z, \theta),$$

with  $\theta \in \mathbb{R}^m$ . The following lemma is well-known; we include its proof and those of the following lemmata in Section 6.

**Lemma 1.** *Let  $f$  be a convex, twice continuously differentiable function  $f: \mathbb{R}^n \rightarrow \mathbb{R}$  and*

$$(4) \quad f_{2,\theta_0}(\theta) = f(\theta_0) + \nabla f(\theta_0)(\theta - \theta_0) + (\theta - \theta_0)^T \nabla^2 f(\theta_0)(\theta - \theta_0)$$

*its second order Taylor approximation at  $\theta_0$ . Then  $f_{2,\theta_0}$  assumes its minimum at*

$$(5) \quad \hat{\theta} = \arg \min_{\theta} f_{2,\theta_0}(\theta) = \theta_0 - [\nabla^2 f(\theta_0)]^{-1} \nabla f(\theta_0) .$$

Let  $Z$  be as in (1), set  $\epsilon = (\epsilon_z)_{z \in Z}$ , and define the function  $u_\epsilon(\theta)$  by

$$(6) \quad u_\epsilon(\theta) = f_Z(\theta) + \sum_{z \in Z} \epsilon_z L(z, \theta) ,$$

where we by construction have  $u_0(\theta) = f_Z(\theta)$ . The function  $u_\epsilon$  can be thought of as an  $\epsilon$ -deformation of  $f_Z$  at 0. We set  $\hat{\theta}_{u_\epsilon} = \arg \min_{\theta} u_\epsilon(\theta)$ , which depends on  $\epsilon$ , note that  $\hat{\theta}_{u_0} = \hat{\theta}_{f_Z} = \hat{\theta}$ , and write  $H = \nabla^2 f_Z(\hat{\theta})$  for the Hesse matrix of  $f_Z$  at  $\hat{\theta}$ . In the following, we will drop  $\epsilon$  from  $u_\epsilon$  and simply write  $u$  when it is clear from the context.

**Lemma 2.**

$$(7) \quad \frac{\partial}{\partial \epsilon_z} \hat{\theta}_{u_0} = -H^{-1} \nabla L(z, \hat{\theta}) .$$

In the following, it is convenient to introduce the symmetric, positive definite, bi-linear form  $\beta_f$  given by

$$\beta_f(v, w) = \langle v, w \rangle = v^T H^{-1} w .$$

**Lemma 3.**

$$\begin{aligned} \frac{\partial}{\partial \epsilon_z} L(z', \hat{\theta}_{u_0}) &= -\nabla L(z', \hat{\theta})^T [\nabla^2 f(\hat{\theta})]^{-1} \nabla L(z, \hat{\theta}) \\ \frac{\partial}{\partial \epsilon_z} L(z', \hat{\theta}_{u_0}) &= -\langle \nabla L(z', \hat{\theta}), \nabla L(z, \hat{\theta}) \rangle = \frac{\partial}{\partial \epsilon_{z'}} L(z, \hat{\theta}_{u_0}) \end{aligned}$$

The  $z/z'$  symmetry in the latter expression has, to our knowledge, not been previously stated and will be of particular relevance for the proof of the main result.

### 3. MAIN RESULTS

Let  $Z = \{z_1, \dots, z_n\}$  be a sample as in (1) and introduce

$$X_u(\{z, z'\}) = \frac{\partial}{\partial \epsilon_z} L(z', \hat{\theta}_u)$$

which is well-defined by Lemma 3 since  $\frac{\partial}{\partial \epsilon_z} L(z', \hat{\theta}) = \frac{\partial}{\partial \epsilon_{z'}} L(z, \hat{\theta})$ . We are interested in studying what happens when a subset  $M \subset Z$  is removed from  $Z$ . To this end, let  $|M| = s \leq n = |Z|$  and define  $\eta_M = (\epsilon_t)_t$  by

$$\epsilon_t = \begin{cases} -1/n , & \text{if } t \in M \\ 0 , & \text{otherwise,} \end{cases}$$

and thus

$$u_{\eta_M}(\theta) = f_Z(\theta) - \sum_{t \in M} \frac{1}{n} L(t, \theta) .$$

Note that the loss function with respect to  $Z \setminus M$  is  $f_{Z \setminus M}(\theta) = \frac{1}{n-s} \sum_{t \in Z \setminus M} L(t, \theta)$  is different from the function

$$u_{\eta_M}(\theta) = \frac{1}{n} \sum_{t \in Z \setminus M} L(t, \theta),$$

derived from  $f_Z(\theta)$  by removing all terms  $L(t, \theta)$  for  $t \in M$ . However, for any constant  $\alpha > 0$  we have  $\arg \min_{\theta} f = \arg \min_{\theta} (\alpha f)$  and thus

$$\arg \min_{\theta} f_{Z \setminus M} = \arg \min_{\theta} u_{\eta_M},$$

that is,  $f_{Z \setminus M}$  assumes a minimum at  $\hat{\theta}_{u_{\eta_M}}$ . With  $f_{Z \setminus M}$  we have associated loss terms  $L(z', \hat{\theta}_{u_{\eta_M}})$  which are exhibiting a different model, specific to the set  $M$  of data points being removed. Accordingly we have the random variable

$$X_{u_0} = \frac{\partial}{\partial \epsilon_z} L(z', \hat{\theta}_{u_0})$$

describing the original system with twice continuously differentiable convex loss function  $f_Z(\hat{\theta}_{u_0}) = \frac{1}{n} \sum_t L(t, \hat{\theta}_{u_0})$ , and the random variable

$$X_{u_{\eta_M}} = \frac{\partial}{\partial \epsilon_z} L(z', \hat{\theta}_{u_{\eta_M}}),$$

describing the systems where the data set  $M$  has been removed with loss functions  $f_{Z \setminus M}(\hat{\theta}_{u_{\eta_M}}) = \frac{1}{n-s} \sum_t L(t, \hat{\theta}_{u_{\eta_M}})$ . We view the moments

$$\mathbb{E}[X_u^k] = \frac{1}{\binom{n}{2}} \sum_{\substack{\{z, z'\}, z \neq z' \\ z, z' \in Z}} \left[ \frac{\partial}{\partial \epsilon_z} L(z', \hat{\theta}_{u_{\eta_M}}) \right]^k$$

as an influence potential of a data set  $Z$  for given loss function  $f_Z(\theta)$  having its minimum at  $\hat{\theta}_{u_{\eta_M}}$ .

**Theorem 1.** *Let  $M \subset Z$  with  $|M| = s$ , where  $s \leq n_0$ , and  $n$  is sufficiently large. Furthermore, let  $X_{u_0}, X_{u_{\eta_M}}$  be the random variables  $X_{u_0}(\{z, z'\}) = \frac{\partial}{\partial \epsilon_z} L(z', \hat{\theta}_{u_0})$  and  $X_{u_{\eta_M}}(\{z, z'\}) = \frac{\partial}{\partial \epsilon_z} L(z', \hat{\theta}_{u_{\eta_M}})$ , respectively. Then*

$$(8) \quad \mathbb{E}[X_{u_0}^k] - \frac{1}{\binom{n}{s}} \sum_{\substack{M \subset Z \\ |M|=s}} \mathbb{E}[X_{u_{\eta_M}}^k] = \frac{ks}{n-2} \mathbb{E}[X_{u_0}^k] + O(n^{-2}).$$

The full proof is given in Section 6 on page 20; here we provide an outline of the main arguments.

We view  $\left[ \frac{\partial}{\partial \epsilon_z} L(z', \hat{\theta}_u) \right]^k$  as a function of  $\epsilon = (\epsilon_t)_t$ , form its Taylor expansion at  $(\epsilon_t)_t = 0$ , and subsequently evaluate at  $\epsilon = \eta_M$ . Next we consider pairs  $(M, \{z', z\})$  where  $z, z' \notin M$ .

Summing over all pairs  $(M, \{z', z\})$  we provide interpretations of the key expressions

$$\begin{aligned} \frac{1}{\binom{n-2}{s}} \frac{1}{\binom{n}{2}} \sum_{\substack{(M, \{z', z\}) \\ |M|=s}} \left[ \frac{\partial}{\partial \epsilon_z} L(z', \hat{\theta}_{u_0}) \right]^k &= \mathbb{E}[X_{u_0}^k] \\ \frac{1}{\binom{n-s}{2}} \sum_{\{z, z'\} \cap M = \emptyset} \left[ \frac{\partial}{\partial \epsilon_z} L(z', \hat{\theta}_{u_{\eta_M}}) \right]^k &= \mathbb{E}[X_{u_{\eta_M}}^k], \end{aligned}$$

as well as

$$\frac{1}{\binom{n}{s}} \frac{1}{\binom{n-s}{2}} \sum_{\substack{(M, \{z', z\}) \\ |M|=s}} \left[ \frac{\partial}{\partial \epsilon_z} L(z', \hat{\theta}_{u_{\eta_M}}) \right]^k = \frac{1}{\binom{n}{s}} \sum_{\substack{M \subset Z \\ |M|=s}} \mathbb{E}[X_{u_{\eta_M}}^k].$$

Since  $f_{Z \setminus M}$  assumes a minimum at  $\hat{\theta}_{u_{\eta_M}}$  we derive from these interpretations

$$\begin{aligned} \Delta_s(\mathbb{E}[X_{u_0}^k]) &= \rho_s \sum_{(M, \{z', z\})} \left[ \frac{\partial}{\partial \epsilon_z} L(z', \hat{\theta}_{u_0}) \right]^k - \left[ \frac{\partial}{\partial \epsilon_z} L(z', \hat{\theta}_{u_{\eta_M}}) \right]^k \\ &= k \rho_s \sum_{\{z, z'\}} \left[ \left[ \frac{\partial}{\partial \epsilon_z} L(z', \hat{\theta}_{u_0}) \right]^{k-1} \left[ \sum_M \sum_{y \in M} \left[ \frac{\partial^2}{\partial \epsilon_y \partial \epsilon_z} L(z', \hat{\theta}_{u_0}) \cdot \left( \frac{1}{n} \right) + O(n^{-2}) \right] \right] \right]. \end{aligned}$$

We then observe that the inner double sum on the RHS simplifies to

$$(9) \quad \binom{n-3}{s-1} \sum_{\substack{y \in Z \\ y \neq z, z'}} \left[ \frac{\partial^2}{\partial \epsilon_y \partial \epsilon_z} L(z', \hat{\theta}_{u_0}) \left( \frac{1}{n} \right) + O(n^{-2}) \right]$$

which allows us employ Lemma 7 and subsequently derive

$$\begin{aligned} \Delta_s(\mathbb{E}[X_{u_0}^k]) &= \mathbb{E}[X_{u_0}^k] - \frac{1}{\binom{n}{s}} \sum_{\substack{M \subset Z \\ |M|=s}} \mathbb{E}[X_{u_{\eta_M}}^k] \\ &= \frac{ks}{n-2} \mathbb{E}[X_{u_0}^k] + \frac{ks}{n-2} O(n^{-1+2-2}). \end{aligned}$$

It is worth noting that in case of the removal of large sets  $M$ , say  $|M| = O(n)$ , the  $M$ -indexed Taylor expansion, as detailed in Equation (18) of Section 6, does not produce information about individual,  $M$ -indexed terms  $\left[ \frac{\partial}{\partial \epsilon_z} L(z', \hat{\theta}_{u_{\eta_M}}) \right]^k$  since the total differential involves  $O(n)$  terms and the quadratic term error term in Equation (18) becomes a constant.

Theorem 1 is concerned with the average over all such  $M$ -indexed terms and as the proof shows these averages,  $\frac{1}{\binom{n}{s}} \sum_{\substack{M \subset Z \\ |M|=s}} \mathbb{E}[X_{u_{\eta_M}}^k]$ , are expressed via Equation (19), see Section 6 for details, as multiples of a sum over all  $y \in Z$ ,  $y \neq z, z'$ . The condition  $s \leq n_0$  and  $n$  being sufficiently large assures that the Taylor expansion approximation of  $\left[ \frac{\partial}{\partial \epsilon_z} L(z', \hat{\theta}_{u_{\eta_M}}) \right]^k$  and in particular the quadratic error term in Equation (18) are well-defined.

The following statements represent basic facts needed to prove Lemma 6, which in turn implies Lemma 7.

**Lemma 4.**

$$\frac{\partial^2}{\partial \epsilon_z \partial \epsilon_x} \hat{\theta}_{u_0} = H^{-1} \left[ \nabla^2 L(z, \hat{\theta}) \right] H^{-1} \cdot \nabla L(x, \hat{\theta}) + H^{-1} \left[ \nabla^2 L(x, \hat{\theta}) \right] H^{-1} \cdot \nabla L(z, \hat{\theta}).$$

(Proof on page 18.)

**Lemma 5.**

$$\begin{aligned} \frac{\partial^2}{\partial \epsilon_x \partial \epsilon_z} L(z', \hat{\theta}_{u_0}) &= -\left\langle \frac{\partial}{\partial \epsilon_z} \nabla L(z', \hat{\theta}_{u_0}), \nabla L(x, \hat{\theta}_{u_0}) \right\rangle + \\ &\quad \left\langle \nabla L(z', \hat{\theta}_{u_0}), \nabla^2 L(x, \hat{\theta}_{u_0}) H_{u_0}^{-1} \nabla L(z, \hat{\theta}_{u_0}) \right\rangle + \\ &\quad \left\langle \nabla L(z', \hat{\theta}_{u_0}), \nabla^2 L(z, \hat{\theta}_{u_0}) H_{u_0}^{-1} \nabla L(x, \hat{\theta}_{u_0}) \right\rangle \end{aligned}$$

(Proof on page 18.)

**Lemma 6.**

$$(10) \quad \frac{1}{n} \sum_{y \in Z} \frac{\partial^2}{\partial \epsilon_y \partial \epsilon_z} L(z', \hat{\theta}_{u_0}) = \frac{\partial}{\partial \epsilon_z} L(z', \hat{\theta}_{u_0}).$$

(Proof on page 19.)

**Lemma 7.** For any fixed pair  $z' \neq z$ ,  $z, z' \in Z$  holds

$$(11) \quad \sum_{y \in Z, y \neq z, z'} \left[ \frac{\partial^2}{\partial \epsilon_y \partial \epsilon_z} L(z', \hat{\theta}_{u_0}) \left( \frac{1}{n} \right) + O(n^{-2}) \right] = \frac{\partial}{\partial \epsilon_z} L(z', \hat{\theta}_{u_0}) + O(n^{-1}).$$

(Proof on page 20.) With the help of Theorem 1 we are now in position to formulate our main result:

**Theorem 2.** Let  $M \subset Z$  with  $|M| = s$ , where  $s \leq n_0$  and  $n$  is sufficiently large. Let  $X_{u_0}$  and  $X_{u_{\eta_M}}$  be the random variables expressing the influence between data-points  $z, z'$  in  $Z$  and  $Z \setminus M$ , respectively. Then we have

$$(12) \quad \mathbb{V}[X_{u_0}] - \frac{1}{\binom{n}{s}} \sum_{\substack{M \subset Z \\ |M|=s}} \mathbb{V}[X_{u_{\eta_M}}] = \frac{2s}{n-2} \mathbb{V}[X_{u_0}] + O(n^{-2}).$$

(Proof on page 22.)

The following corollary of Theorem 2 is the cornerstone of this paper. It establishes that a descent on the variance  $\mathbb{V}[X]$  is always possible, subject to certain data size conditions.

**Corollary 1.** Suppose we are given a data set  $Z$  and a twice differentiable, convex loss function  $f_Z(\theta) = \frac{1}{n} \sum_z L(z, \theta)$  with a minimum at  $\hat{\theta}$  and potential  $0 < \mathbb{E}[X_{u_0}^k]$ . Then for  $s \leq n_0$  and sufficiently large  $n$ , there exists a subset  $M_0 \subset Z$  with  $|M_0| = s$  such that

$$(13) \quad \frac{2s}{n-2} \mathbb{E}[X_{u_0}^k] + O(n^{-2}) \leq \mathbb{E}[X_{u_0}^k] - \mathbb{E}[X_{u_{\eta_{M_0}}}^k].$$

Furthermore

$$(14) \quad \frac{2s}{n-2} \mathbb{V}[X_{u_0}] + O(n^{-2}) \leq \mathbb{V}[X_{u_0}] - \mathbb{V}[X_{u_{\eta_{M_0}}}]$$

(Proof on page 22.)

## 4. APPLICATIONS

In this section we present two proof-of-concept case studies that put the following two conjectures to the test:

- (a) variance encapsulates data heterogeneity and inversely correlated to test accuracy, and
- (b) variance-based removal of sample points causes a drop in variance and an increase in test accuracy.

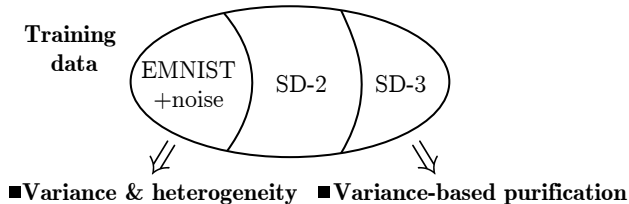


FIGURE 2. Outline: three classes of data each analyzed with respect to variance, heterogeneity, test accuracy and subjected to variance-based purification. SD-2 and SD-3 denote synthetic data containing two and three distinct distributions, respectively.

As depicted in Figure 2, our experiments involve three classes of data: a subset of the EMNIST data [6] and two varieties of a synthetic data set. For the EMNIST data, samples of given sizes containing two distribution are constructed through mislabeling a certain fraction  $r$  of the training data. (The two distributions being represented by the correctly labeled images and the incorrectly labeled images.) For the synthetic data, denoted by SD- $K$  and described below, we synthesize training data of prescribed sizes containing a specified number  $K$  of distributions at prescribed ratios. Each data set is then probed using the following experiments: (1) tracking of the variance  $\mathbb{V}[X]$  and test accuracy as a function of the composition ratio of the distributions, and (2) measurements of the variance  $\mathbb{V}[X]$  and testing accuracy under variance-based sample point removals. We note that while high accuracy can always be achieved on the training set by increasing model complexity or extending the number of training epochs, high accuracy on the independent test set reflects the model’s true predictive capability. Test accuracy thus serves as a reliable benchmark for assessing the predictive power and generalization ability of a trained model. In each case, multinomial logistic regression (MLR) was employed using the PyTorch [24] library and its ADAM optimizer with parameters as detailed below. We remark that these are preliminary experiments meant to illustrate our framework, and refer to Section 5 for a discussion of implications, use of deep learning architectures, and design of engineering principles and algorithms targeting scaling and generalization.

**Data description.** For the EMNIST data [6] we used all 10 digits, each represented by  $10^3$  data points for a total sample size of  $|Z| = 10^4$  distributed evenly for each digit. The synthetic data sets are constructed using a family of functions defined in the following manner. Each function is of the form  $\phi^\ell: E^{10} \rightarrow E$  for the alphabet  $E = \{R, D, B, N\}$ , and is defined in terms of positional real-valued weights  $q^\ell = (q_i^\ell)_{i=1}^{10}$  (i.e., feature weights),

alphabet weights  $w^\ell = (w_i^\ell)_{i \in E}$ , and thresholds  $a^\ell = (a_i^\ell)_{i=1,2,3}$  by

$$(15) \quad \phi^\ell(x) = \begin{cases} R, & \text{if } C(x) \leq a_1, \\ D, & \text{if } a_1 < C(x) \leq a_2, \\ B, & \text{if } a_2 < C(x) \leq a_3, \\ N, & \text{if } a_3 < C(x). \end{cases}$$

where  $C(x) = \sum_{i=1}^{10} q_i^\ell w^\ell(x_i)$ . A sample  $Z$  of size  $N = N_1 + N_2 + \dots + N_K$  is constructed as the union of sets whose  $N_i$  elements are pairs  $(x, \phi^i(x))$  where the feature vectors  $x$  are sampled from  $U(E^{10})$ . The specific distribution parameters are given as follows:

label\_weights\_1: R: 1.0, D: -1.0, N: 0.3, B: -0.3

label\_weights\_2: R: -0.4, D: 1.0, N: -0.8, B: 0.6

label\_weights\_3: R: 1.2, D: 0.4, N: -0.2, B: -0.8

feature\_weights\_1: [ 1, -1, 1, -1, 1, -1, 1, -1, 1, -1]

feature\_weights\_2: [0.5, 0.5, -1, 1, 0, -0.5, 1, -1, 0.5, -0.5]

feature\_weights\_3: [ 1, 0.5, 1, 1, 0.5, -0.5, -1, -1.5, -0.5, 1]

threshold\_1: a\_3=2.0, a\_2=0.0, a\_1=-2.0

threshold\_2: a\_3=1.5, a\_2=0.0, a\_1=-1.5

threshold\_3: a\_3=2.0, a\_2=0.0, a\_1=-2.5

**4.1. EMNIST image data.** We provide next our findings about relating variance with data heterogeneity and test accuracy as well as the effect of variance-based purification. We display variance and predication accuracy relation as a combination of the mixing ratio of correctly and incorrectly labeled EMNIST image data, and the effect of variance based removal of certain training points. In Figure 3, we showcase variance  $\mathbb{V}[X]$  and accuracy as functions of the error rate  $r$ .

We proceed by illustrating how the variance  $\mathbb{V}[X]$  can be used to improve prediction accuracy through elimination of sample points under MLR. For the case shown in Figure 4 we again used EMNIST data, but this time with  $|Z| = 1200$  images composed of  $n_4 = 600$  digits '4' and  $n_8 = 600$  digits '8'. The sample  $Z$  was split into a training set  $A_1$  with  $|A_1| = 600$ , with each digit evenly distributed, and a test set  $A_2$  with  $|A_2| = 1200 - |A_1| = 600$ , and for the training set  $A_1$  we randomly mislabeled a fraction  $r = 0.30$  of the points. Finally, after initial training we measure the initial variance  $\mathbb{V}[X]$  and testing accuracy, corresponding to the values for iteration 0 in Figure 4.

Next we iterated the following procedure: for each  $z \in A_1 = A_1^0$  train the MLR model on  $A_{1,-z}^0 = A_1^0 \setminus z$ , aka leave-one-out (LOO), and record test accuracy. Following this, measure

$$\delta(z, A_1^0) = \mathbb{V}[A_1^0] - \mathbb{V}[A_{1,-z}^0],$$

and then remove the  $k = 10$  points of  $A_1^0$  with the largest value of  $\delta$  to obtain  $A_1^1$ , concluding iteration 1. The MLR model is then retrained on  $A_1^1$ ,  $k = 10$  points are removed mapping  $A_1^1$  into  $A_1^2$ , and so on.

Figure 4, shows that variance drops quickly until about iteration 4 while the test accuracy steadily increases for about 20 iterations which corresponds to removal of 200 sample points from  $A_1^0$  (shown by vertical dashed line). This ‘‘purification’’ procedure identifies a subset  $A_1' \subset A_1$  that allows for a significantly higher test accuracy despite  $|A_1'| < |A_1|$ .

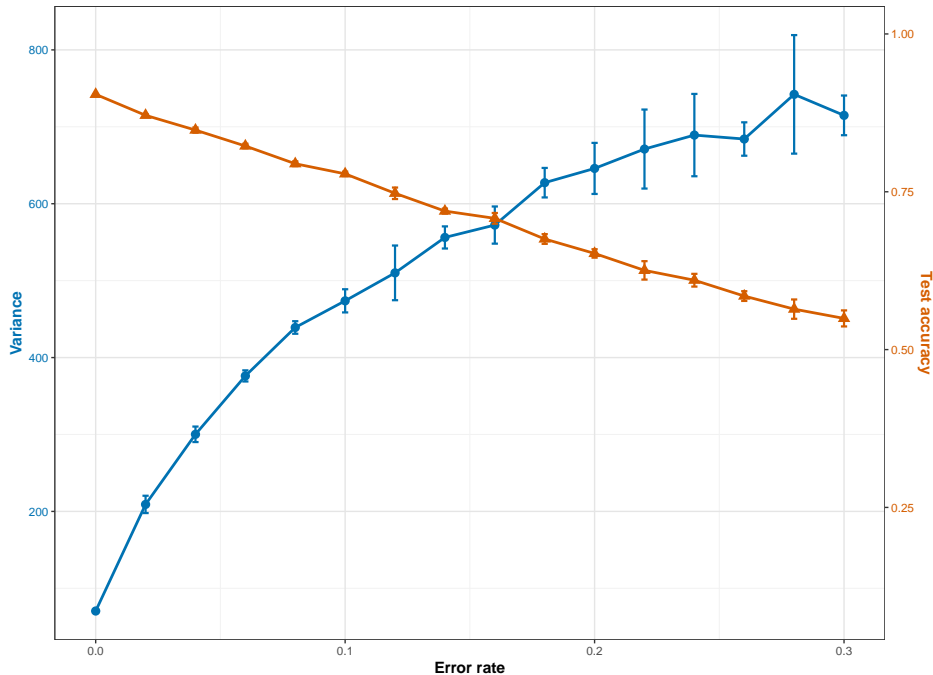


FIGURE 3. Variance  $\mathbb{V}[X]$  (blue curve) and prediction accuracy (orange curve) for EMNIST data as a function of the error rate  $r$  applied to training data. All 10 digits were used, with each digit 0 through 9 represented by  $10^3$  images to obtain  $|Z| = 10^4$ . We train an MLP model which takes all  $28 \times 28$  gray scale pixels as features, with learning rate  $10^{-3}$  and batch size 64, and use the trained model to predict on a disjoint test set of size  $10^4$  sampled from EMNIST data. The horizontal axis gives the error rate, and the left (resp. right) vertical axis gives the variance  $\mathbb{V}[X]$  (resp. test accuracy). Filled circles/triangles show expectations, while bars show standard deviations across the 5 replications generated for each error rate  $r$ . Note that the error rates for test accuracy are small and that nearly all error bars are contained inside the triangle showing the expectation.

**4.2. Synthetic data - two distributions.** Using synthetic data induced by two distributions and a total sample size  $|Z| = 600$  and MLR, Figure 5 indicates a clear pattern: data heterogeneity negatively impacts prediction accuracy, and the variance,  $\mathbb{V}[X]$ , correlates positively with heterogeneity. Here accuracy reaches a minimum near the 50/50 mix, at which point the potential reaches its maximal value.

Figure 6 represents the analogue of Figure 4 which shows the variance-based, iterated purification using Leave-One-Out under MLR as detailed in the previous section for a sample  $Z$  consisting of  $10^3$  points. Note that at iteration 100, all data points would have been removed. One may speculate regarding the relation between the maximal test accuracy and the inflection point in the variance.

**4.3. Synthetic data - three distributions.** It is natural to ask how the observations from the previous two sections translate to a sample where three or more distributions are present. Referring to Figure 7 we illustrate the variance  $\mathbb{V}[X]$  under MLR for a 3-distribution synthetic

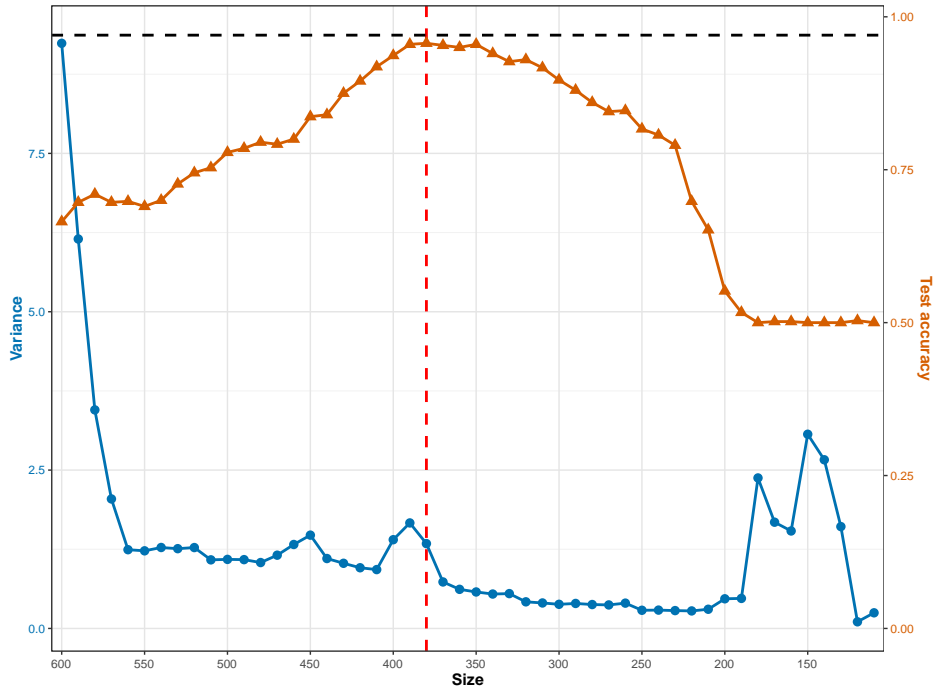


FIGURE 4. The evolution of training set variance  $\mathbb{V}[X]$  (blue curve) and test accuracy (orange curve) over 20 purification iterations. Here a training set  $T$  consists of 600 EMNIST samples digits '4' and '8' (evenly distributed) with an error rate  $r = 0.30$ . An independent test set  $S$  contains 600 correctly labeled EMNIST samples with the same digit distributions as  $T$ . Training was conducted using MRL with batch size 64 and learning rate  $10^{-3}$ . For reference, we trained a model on a single distribution training set  $T_0$  of size 600, evaluated on  $S$ , obtaining a test accuracy of 0.97 at  $r = 0$ , shown as the dashed black line. The maximal accuracy reached during purification was 0.957 which occurred when 220 data points had been removed, shown at the red dashed line.

data where the sample  $Z$  is fixed at size 600, and where the three distributions are denoted by  $A_1$ ,  $A_2$ , and  $A_3$ . The projections onto the planes  $|A_2| = 0$  and  $|A_3| = 0$  clearly match the structure of the variance shown in Figure 5. It also appears that variance captures the degree of heterogeneity being larger near the “diagonal” where  $|A_1| = |A_2| = |A_3|$ .

Similarly, in Figure 8 we show variance-based LOO purification for a 700/150/150 mixed 3-distribution synthetic data sample  $Z$  using MLR. Again we observe a steady increase in test accuracy and a steady drop in variance  $\mathbb{V}[X]$  for about 20 iterations. Here test accuracy ranges from about 0.65 for the initial sample  $Z$  to almost 0.85 upon targeted removal of about 20% of the sample points. One also notices that test accuracy peaks near the inflection point of the variance.

## 5. DISCUSSION

In this paper we have introduced a system-level random variable  $X$  representing the influences among all training data points. Its basic properties allow characterization and

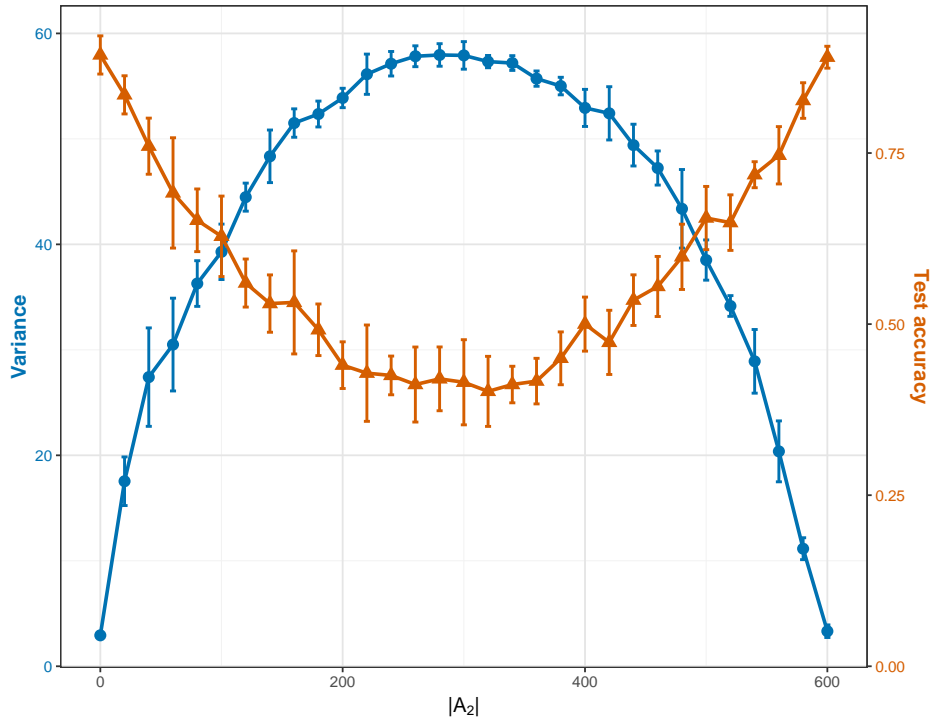


FIGURE 5. Variance  $\mathbb{V}[X]$  and test accuracy as functions of mixed synthetic data (SD-2) with two distributions  $(A_1, A_2)$  and  $|Z| = 600$  using MLR. The horizontal axis shows  $|A_2|$  with  $|A_1| = |Z| - |A_2|$ . The left vertical axis shows test variance (blue curve) while the right axis shows the test accuracy (orange curve).  $Z$  is randomly split into training and test sets in an 8:2 ratio. The test accuracy is computed by training the model on the training set and evaluating it on the test set. Filled circles/triangles give the expectations while error bars show standard deviations; for each composition  $k = 5$  replications were generated. For the MLR training batch size was 64 and learning rate was  $10^{-3}$ .

manipulation of ensemble properties, supporting the goal of improving prediction accuracy. This perspective has immediate implications: random variables are understood via their moments which become central to our framework. The question then becomes: can we insights on moments to deeper insights into the structure of training data? Assuming convexity, Theorems 1 and 2 show that the second centered moment  $\mathbb{V}[X]$  can support a form of data purification in which sub-samples of data are produced that reduce variance. Theorem 2 and its corollary are tantamount to an existence proof of a purification algorithm, immediately raising two questions: (a) how does variance relate to data heterogeneity, and (b) can we construct efficient variance-based algorithms that produce subsets of data on which prediction accuracy is improved?

To ground our statements and results, we need to make precise what we mean by data heterogeneity. Here heterogeneity is relative to the context within which the set data  $Z$  is analyzed: it depends on the choice of machine learning architecture and loss function, with a loss function implying that training points are of the form  $z = (x, y)$ . This context

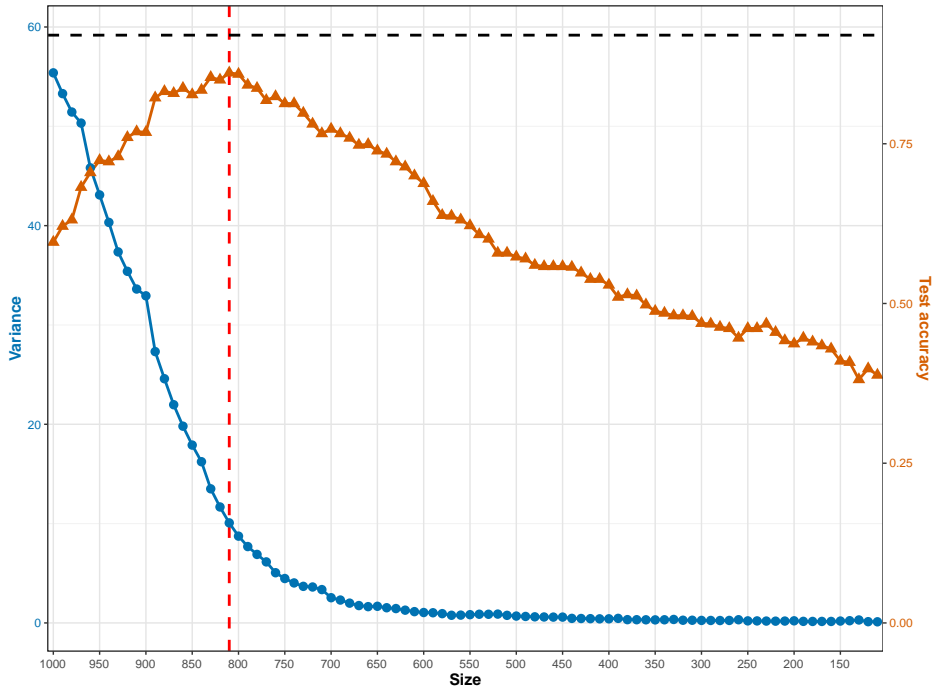


FIGURE 6. Evolution of training set variance  $\mathbb{V}[X]$  (blue curve) and test accuracy (orange curve) over 20 purification steps using synthetic data SD-2 and MRL. Here the SD-2 training set  $Z$  is composed of distributions  $A_1$  and  $A_2$  with  $|A_1| = 700$  and  $|A_2| = 300$ ; the test set  $S$  consists of 1000 data points following the distribution  $A_1$ . Training was conducted using MRL with batch size 64 and learning rate 0.001. For reference, we trained a model on a set  $Z_0$  consisting of  $10^3$  data points following distribution  $A_1$  and evaluated on  $S$  obtaining a test accuracy is 0.94 (black dashed line). During purification, the maximal test accuracy was measured to be 0.86 occurring after removal of 190 data points (red dashed line).

determines what we can infer from the data, and determines which distributions we can recognize.

Suppose we fix the context and that  $\ell$  different distributions are present in the data where distributions are represented by functions  $f_i: X \rightarrow Y$ . heterogeneity is tantamount to the entropy

$$E(Z) = - \sum_{i=1}^{\ell} p_i \log(p_i) ,$$

where  $p_i$  denotes the fraction of data consistent with function  $f_i$ . Clearly, if only one function is present we have  $E(Z) = 0$  which is minimal, and one may call the system pure. On the other hand,  $E(Z)$  is maximal with value  $\log(\ell)$  if for given  $\ell \geq 2$  the data points are uniformly distributed among the  $\ell$  blocks. Random data represents the extreme case where each data point represents its own distribution and heterogeneity is maximized at  $\log(|Z|)$ .

Given a context and an unknown training set  $Z$  we cannot directly infer its heterogeneity, which is why we introduced the variance which can be used as a proxy for this. By design,

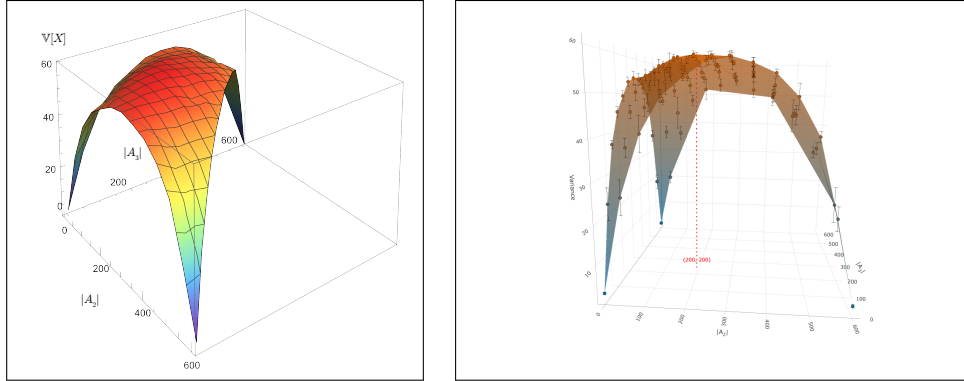


FIGURE 7. Variance  $\mathbb{V}[X]$  as a function of sample composition for SD-3 where  $|Z| = |A_1| + |A_2| + |A_3| = 600$ . Variance ( $z$ -axis) is shown as a function of  $(|A_2|, |A_3|)$  where  $|A_2|$  and  $|A_3|$  are shown on the  $x$ - and  $y$ -axis, respectively. Here MLR was used with the synthetic SD-3 data. On the right, filled circles represent expectations and error bars encode standard deviations. Each data point was generated using  $k = 5$  replications. For the MLR training the batch size was 64 and the learning rate was 0.001. The variance peaks at  $|A_1| = |A_2| = |A_3| = 200$  as indicated by the red dashed line on the right.

we knew the composition of the data in all our experiments in Section 4, which allowed us to showcase the relation between variance and heterogeneity, demonstrated in Figures 3, 5, and 7 where  $\mathbb{V}[X]$  faithfully captures data heterogeneity. Figure 4 shows that removing “noise” from the image data leads to a drop in  $\mathbb{V}[X]$ . Obviously, this also decreases entropy by increasing the fraction of correctly labeled image data. In the case of three distributions, Figures 5 and 7 show that  $\mathbb{V}[X]$  assumes its maximum when all functions have equal support within the data, matching the behavior of entropy.

It is not within the scope of this work to present a polished, computational efficient framework for variance-based optimization of prediction accuracy. However, our proof-of-concept examples have demonstrated that variance-based purification via Corollary 1 can lead to significant improvements of test accuracy. This suggests that variance, which is a quantity that can be determined and/or estimated from the training data, supports a principled identification of “outliers”. As can be seen in all the experiments, variance-based purification goes through a regime of increased test accuracy, but eventually transitions into a second regime where additional removal has a negative impact. Here it is important to note that as more and more data points are removed (the case of large  $|M|$ ), we no longer have  $O(n^{-2})$  error terms as stipulated in Theorem 2. From this point onward, finite size effects render variance less and less informative.

The experiments presented here were based on leave-one-out (LOO) with retraining, viable mainly for simpler models and conservatively sized training data. In ongoing work, we are exploring the use of influence (see Lemma 3 and [16, 7]) as a means to identify the sets  $M$  in a computationally cheaper manner. Initial results indicate that this approach works well, including for architectures such as deep neural networks where convexity assumptions fail [18]. Preliminary experiments using DL architectures and variance-based construction of the sets  $M$  (not in this paper) based on retraining show patterns quite similar to those observed in Figures 6 and 8. Since variance as a concept does not depend on convexity, it

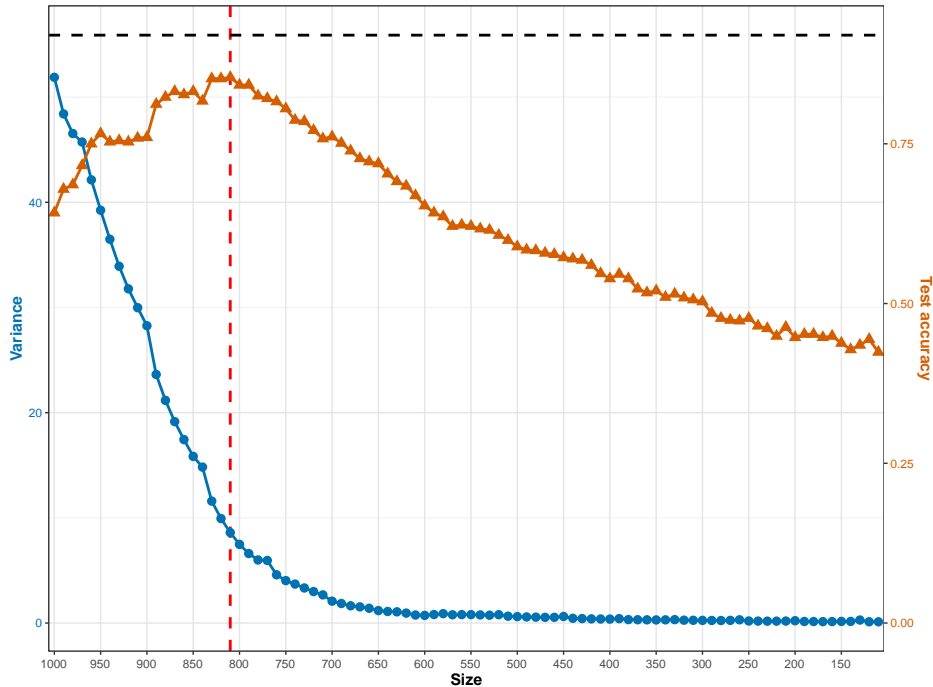


FIGURE 8. The evolution of training set variance  $\mathbb{V}[X]$  (blue curve) and test accuracy (orange curve) over 20 purification steps using synthetic SD-3 data. Here  $Z$  is composed of distributions  $A_1$ ,  $A_2$  and  $A_3$  with  $|A_1| = 700$ ,  $|A_2| = 150$  and  $|A_3| = 150$ . The test set consists of  $10^3$  data points following the distribution  $A_1$ . Training was conducted using MRL with batch size 64 and learning rate  $10^{-3}$ . For reference, we trained a model  $Z_0$  consisting of  $10^3$  data points following the distribution  $A_1$  and evaluated it on  $S$ , obtaining accuracy 0.94 as shown by the black dashed line. The maximal test accuracy observed during purification was 0.86 which occurred after removal of 190 data points (red dashed line).

appears to represent a tool to purify data. [4, 9, 11, 19] show that an analytical approach based on convexity is not applicable. The development of a framework suitable for DL-architectures is work in progress.

In ongoing work we are exploring the engineering of efficient variance-based purification algorithms and stopping criteria for the removal process. Figure 1 shows our vision for how this framework could advance supervised learning. Sample data is subjected to initial training where the purpose is purification rather than prediction. Following this, the data is partitioned into pure blocks followed by separate, local training on each pure block to obtain the sub-models using conventional architectures. Since the blocks are more homogeneous, one may be able to use less complex architectures and still obtain increased accuracy. In this framework, prediction follows the use of a classifier that routes new data to the appropriate sub-model(s).

Finally we are seeking to formally understand how  $\mathbb{V}[X]$  and entropy relate which would bridge this work and the information-theoretic framework developed in [3] for RNA sequence clustering. The fact that  $\mathbb{V}[X]$  mimics the behavior of entropy is likely not a coincidence.

Analysis of higher order moments such as kurtosis is likely to yield additional insight that can support data analysis.

## 6. PROOFS

### 6.1. Proofs of basic facts.

*Proof of Lemma 1.* By convexity of  $f$  it follows that  $f_{2,\theta_0}$  is convex and thus its minimum is attained where  $\nabla f_{2,\theta_0}(\theta) = 0$ . From (4) on page 5 we derive

$$\begin{aligned}\nabla f_{2,\theta_0}(\theta) &= \nabla [\nabla f(\theta_0)^T(\theta - \theta_0)] + \nabla \left[ \frac{1}{2}(\theta - \theta_0)^T \nabla^2 f(\theta_0)(\theta - \theta_0) \right] \\ &= \nabla f(\theta_0) + \nabla^2 f(\theta_0)(\theta - \theta_0),\end{aligned}$$

which, when equated to 0, yields

$$\hat{\theta} = \arg \min_{\theta} f_{2,\theta_0}(\theta) = \theta_0 - [\nabla^2 f(\theta_0)]^{-1} \nabla f(\theta_0).$$

□

*Proof of Lemma 2.* By construction,  $\nabla u_{\epsilon}(\hat{\theta}_{u_{\epsilon}}) = 0$  as  $u_{\epsilon}$  assumes a minimum at  $\hat{\theta}_{u_{\epsilon}}$ . To prove (7) from page 5, we first apply Lemma 1 to  $u_{\epsilon}$  at  $\theta_0 = \hat{\theta}$  leading to

$$(16) \quad \hat{\theta}_u - \hat{\theta} = - \left[ \nabla^2 \left( f(\hat{\theta}) + \sum_t \epsilon_t L(t, \hat{\theta}) \right) \right]^{-1} \nabla \left[ f(\hat{\theta}) + \sum_t \epsilon_t L(t, \hat{\theta}) \right].$$

Since  $\nabla f(\hat{\theta}) = 0$  and  $\nabla [f(\hat{\theta}) + \sum_t \epsilon_t L(t, \hat{\theta})] = \sum_t \epsilon_t \nabla L(t, \hat{\theta})$ , for  $\epsilon = 0$  holds

$$(17) \quad \frac{\partial}{\partial \epsilon_z} \hat{\theta}_{u_0} = - \frac{\partial}{\partial \epsilon_z} \left[ [\nabla^2 u_0(\hat{\theta})]^{-1} \right] \cdot \left[ \sum_t \epsilon_t \nabla L(z, \hat{\theta}) \right]_{\epsilon=0} - [\nabla^2 u_0(\hat{\theta})]^{-1} \cdot \nabla L(z, \hat{\theta}).$$

Clearly, the first term on the right in (17) vanishes since its second factor is zero. For the second term we note that since  $u_0(\theta) = f(\theta)$  and thus have  $[\nabla^2(u_0)]^{-1} = [\nabla^2 f]^{-1} = H_f^{-1} = H^{-1}$  which inserted into (17) yields (7)

$$\frac{\partial}{\partial \epsilon_z} \hat{\theta}_{u_0} = -H^{-1} \nabla L(z, \hat{\theta}).$$

□

*Proof of Lemma 3.* Applying Lemma 2 to  $L(z', \hat{\theta}_u)$  we derive

$$\frac{\partial}{\partial \epsilon_z} L(z', \hat{\theta}_{u_0}) = \left[ \nabla L(z', \hat{\theta}_{u_0}) \right]^T \frac{\partial}{\partial \epsilon_z} \hat{\theta}_{u_0} = -\nabla L(z', \hat{\theta})^T \left[ \nabla^2 f(\hat{\theta}) \right]^{-1} \nabla L(z, \hat{\theta}),$$

and since  $H$  and therefore  $H^{-1}$  is symmetric,

$$\begin{aligned}\frac{\partial}{\partial \epsilon_z} L(z', \hat{\theta}_{u_0}) &= - \left[ \nabla L(z', \hat{\theta})^T \left[ \nabla^2 f(\hat{\theta}) \right]^{-1} \nabla L(z, \hat{\theta}) \right]^T \\ &= - \nabla L(z, \hat{\theta})^T \left[ \nabla^2 f(\hat{\theta}) \right]^{-1} \nabla L(z', \hat{\theta}) \\ &= - \left[ \nabla L(z, \hat{\theta}_{u_0}) \right]^T \frac{\partial}{\partial \epsilon_{z'}} \hat{\theta}_{u_0} \\ &= \frac{\partial}{\partial \epsilon_{z'}} L(z, \hat{\theta}_{u_0}),\end{aligned}$$

concluding the proof.  $\square$

## 6.2. Proofs for main results.

*Proof of Lemma 4.* From the expression for  $\hat{\theta}_u - \hat{\theta}$  from (16) and following the proof of Lemma 2 we employ Lemma 1 for  $\theta_0 = \hat{\theta}$  and  $u(\theta) = f(\theta) + \sum_t \epsilon_t L(t, \theta)$  to obtain  $\hat{\theta}_u - \hat{\theta} = -[\nabla_{\hat{\theta}}^2 u]^{-1} \nabla_{\theta} u$ . Since  $\frac{\partial}{\partial \epsilon_z} \nabla u = \nabla L(z, \hat{\theta})$  we derive

$$\frac{\partial}{\partial \epsilon_z} \hat{\theta}_u = -\frac{\partial}{\partial \epsilon_z} [\nabla^2 u(\hat{\theta})]^{-1} \cdot \nabla u - [\nabla^2 u(\hat{\theta})]^{-1} \cdot \nabla L(z, \hat{\theta}).$$

Differentiating with respect to  $\epsilon_x$  we have  $\frac{\partial}{\partial \epsilon_x} \nabla u = \nabla L(x, \hat{\theta})$  and

$$\begin{aligned} \frac{\partial^2}{\partial \epsilon_x \partial \epsilon_z} \hat{\theta}_u &= -\frac{\partial^2}{\partial \epsilon_x \partial \epsilon_z} [\nabla^2 u(\hat{\theta})]^{-1} \cdot \nabla u - \frac{\partial}{\partial \epsilon_z} [\nabla^2 u(\hat{\theta})]^{-1} \cdot \nabla L(x, \hat{\theta}) \\ &\quad - \frac{\partial}{\partial \epsilon_x} [\nabla^2 u(\hat{\theta})]^{-1} \cdot \nabla L(z, \hat{\theta}) \end{aligned}$$

Setting  $\epsilon = 0$  we have  $\nabla u_0 = 0$  and accordingly

$$\frac{\partial^2}{\partial \epsilon_x \partial \epsilon_z} \hat{\theta}_{u_0} = -\left[ \frac{\partial}{\partial \epsilon_z} [\nabla_{\hat{\theta}}^2 u_0(\hat{\theta})]^{-1} \cdot \nabla L(x, \hat{\theta}) + \frac{\partial}{\partial \epsilon_x} [\nabla^2 u_0(\hat{\theta})]^{-1} \cdot \nabla L(z, \hat{\theta}) \right].$$

Using the identity  $\frac{\partial}{\partial \epsilon_z} (A^{-1}) = -A^{-1} \cdot \frac{\partial}{\partial \epsilon_z} (A) \cdot A^{-1}$ , and setting  $H = \nabla^2(u_0(\hat{\theta}))$  we obtain

$$\begin{aligned} \frac{\partial}{\partial \epsilon_z} [\nabla^2 u_0(\hat{\theta})]^{-1} &= -H^{-1} \cdot \frac{\partial}{\partial \epsilon_z} \left[ \nabla^2 f(\hat{\theta}) + \sum_t \epsilon_t \nabla^2 L(t, \hat{\theta}) \right] \cdot H^{-1} \\ &= -H^{-1} \cdot [\nabla^2 L(z, \hat{\theta})] \cdot H^{-1}, \quad \text{and} \\ \frac{\partial}{\partial \epsilon_x} [\nabla^2 u_0(\hat{\theta})]^{-1} &= -H^{-1} \cdot \frac{\partial}{\partial \epsilon_x} \left[ \nabla^2 f(\hat{\theta}) + \sum_t \epsilon_t \nabla^2 L(t, \hat{\theta}) \right] \cdot H^{-1} \\ &= -H^{-1} \cdot [\nabla^2 L(x, \hat{\theta})] \cdot H^{-1}, \end{aligned}$$

from which the proof follows.  $\square$

*Proof of Lemma 5.* Using Lemma 2 we compute

$$\begin{aligned} \frac{\partial}{\partial \epsilon_x} \frac{\partial}{\partial \epsilon_z} L(z', \hat{\theta}_u) &= \frac{\partial}{\partial \epsilon_x} \left[ (\nabla L(z', \hat{\theta}_u))^T \frac{\partial}{\partial \epsilon_z} \hat{\theta}_u \right] \\ &= \left[ \frac{\partial}{\partial \epsilon_x} \nabla L(z', \hat{\theta}_u) \right]^T \frac{\partial}{\partial \epsilon_z} \hat{\theta}_u + (\nabla L(z', \hat{\theta}_u))^T \frac{\partial}{\partial \epsilon_x} \left[ \frac{\partial}{\partial \epsilon_z} \hat{\theta}_u \right], \end{aligned}$$

and, employing Lemmata 3 and 4, we obtain at  $\epsilon = 0$

$$\begin{aligned} \frac{\partial}{\partial \epsilon_x} \frac{\partial}{\partial \epsilon_z} L(z', \hat{\theta}_{u_0}) &= \left[ \frac{\partial}{\partial \epsilon_x} \nabla L(z', \hat{\theta}_u) \right]^T \frac{\partial}{\partial \epsilon_z} \hat{\theta}_u + \\ &\quad (\nabla L(z', \hat{\theta}))^T \left[ H_{u_0}^{-1} [\nabla^2 L(z, \hat{\theta})] H_{u_0}^{-1} \cdot \nabla L(x, \hat{\theta}) \right. \\ &\quad \left. + H_{u_0}^{-1} [\nabla^2 L(x, \hat{\theta})] H_{u_0}^{-1} \cdot \nabla L(z, \hat{\theta}) \right]. \end{aligned}$$

Since  $\frac{\partial}{\partial \epsilon_x} \frac{\partial}{\partial \epsilon_z} L(z', \hat{\theta}_u) = \frac{\partial}{\partial \epsilon_z} \frac{\partial}{\partial \epsilon_x} L(z', \hat{\theta}_u)$  we derive

$$\begin{aligned} & \left[ \frac{\partial}{\partial \epsilon_x} \nabla L(z', \hat{\theta}_u) \right]^T \frac{\partial}{\partial \epsilon_z} \hat{\theta}_u + \left( \nabla L(z', \hat{\theta}_u) \right)^T \frac{\partial}{\partial \epsilon_x} \left[ \frac{\partial}{\partial \epsilon_z} \hat{\theta}_u \right] = \\ & \left[ \frac{\partial}{\partial \epsilon_z} \nabla L(z', \hat{\theta}_u) \right]^T \frac{\partial}{\partial \epsilon_x} \hat{\theta}_u + \left( \nabla L(z', \hat{\theta}_u) \right)^T \frac{\partial}{\partial \epsilon_z} \left[ \frac{\partial}{\partial \epsilon_x} \hat{\theta}_u \right] \end{aligned}$$

and using  $\frac{\partial}{\partial \epsilon_x} \left[ \frac{\partial}{\partial \epsilon_z} \hat{\theta}_u \right] = \frac{\partial}{\partial \epsilon_z} \left[ \frac{\partial}{\partial \epsilon_x} \hat{\theta}_u \right]$  produces the equality

$$\left[ \frac{\partial}{\partial \epsilon_x} \nabla L(z', \hat{\theta}_u) \right]^T \frac{\partial}{\partial \epsilon_z} \hat{\theta}_u = \left[ \frac{\partial}{\partial \epsilon_z} \nabla L(z', \hat{\theta}_u) \right]^T \frac{\partial}{\partial \epsilon_x} \hat{\theta}_u.$$

By Lemma 2 holds

$$\left[ \frac{\partial}{\partial \epsilon_z} \nabla L(z', \hat{\theta}_u) \right]^T \frac{\partial}{\partial \epsilon_x} \hat{\theta}_u = - \left\langle \frac{\partial}{\partial \epsilon_z} \nabla L(z', \hat{\theta}_u), \nabla L(x, \hat{\theta}_u) \right\rangle$$

and the lemma follows.  $\square$

*Proof of Lemma 6.* We consider  $\sum_{y \in Z} \frac{\partial^2}{\partial \epsilon_y \partial \epsilon_z} L(z', \hat{\theta}_u)$  and interpret the terms with the help of Lemma 5. The lemma shows that each of these terms is in fact the sum of three values of the bilinear form,  $\langle w, v \rangle = w^T H^{-1} v$ , such that  $y$  only appears in the second variable. Using bilinearity,  $\sum_{y \in Z} \nabla^2 L(y, \hat{\theta}_{u_0}) = nH$  and  $\nabla f_Z(\hat{\theta}_{u_0}) = 0$ , we obtain for the sum of the first terms

$$\begin{aligned} - \sum_{y \in Z} \left\langle \frac{\partial}{\partial \epsilon_z} \nabla L(z', \hat{\theta}_{u_0}), L(y, \hat{\theta}_{u_0}) \right\rangle &= \left\langle \frac{\partial}{\partial \epsilon_z} \nabla L(z', \hat{\theta}_{u_0}), \sum_{y \in Z} \nabla L(y, \hat{\theta}_{u_0}) \right\rangle \\ &= n \left\langle \frac{\partial}{\partial \epsilon_z} \nabla L(z', \hat{\theta}_{u_0}), \nabla f_Z(\hat{\theta}_{u_0}) \right\rangle = 0. \end{aligned}$$

The sum of the second terms is given by

$$\sum_{y \in Z} \left\langle \nabla L(z', \hat{\theta}_{u_0}), \nabla^2 L(y, \hat{\theta}_{u_0}) H^{-1} \nabla L(z, \hat{\theta}_{u_0}) \right\rangle = \left\langle \nabla L(z', \hat{\theta}_{u_0}), \sum_{y \in Z} \nabla^2 L(y, \hat{\theta}_{u_0}) \left( H^{-1} \nabla L(z, \hat{\theta}_{u_0}) \right) \right\rangle.$$

Here  $\nabla^2 L(y, \hat{\theta}_{u_0})$  is an  $m \times m$  matrix and since  $m \times m$  matrices form an algebra we can consider the  $m \times m$  matrix  $\sum_{y \in Z} \nabla^2 L(y, \hat{\theta}_{u_0})$  where  $(\sum_i A_i)x = \sum_i (A_i x)$ . Accordingly we derive

$$\begin{aligned} \sum_{y \in Z} \left\langle \nabla L(z', \hat{\theta}_{u_0}), \nabla^2 L(y, \hat{\theta}_{u_0}) H^{-1} \nabla L(z, \hat{\theta}_{u_0}) \right\rangle &= \left\langle \nabla L(z', \hat{\theta}_{u_0}), \left[ \sum_{y \in Z} \nabla^2 L(y, \hat{\theta}_{u_0}) \right] H^{-1} \nabla L(z, \hat{\theta}_{u_0}) \right\rangle \\ &= n \left\langle \nabla L(z', \hat{\theta}_{u_0}), \nabla L(z, \hat{\theta}_{u_0}) \right\rangle, \end{aligned}$$

since  $HH^{-1}$  is the identity matrix. Finally we use linearity of  $\nabla^2 L(z, \hat{\theta}_{u_0}) H^{-1}$  and conclude

$$\begin{aligned} \sum_{y \in Z} \left\langle \nabla L(z', \hat{\theta}_{u_0}), \nabla^2 L(z, \hat{\theta}_{u_0}) H^{-1} \nabla L(y, \hat{\theta}_{u_0}) \right\rangle &= \left\langle \nabla L(z', \hat{\theta}_{u_0}), \nabla^2 L(z, \hat{\theta}_{u_0}) H^{-1} \left[ \sum_{y \in Z} \nabla L(y, \hat{\theta}_{u_0}) \right] \right\rangle \\ &= n \left\langle \nabla L(z', \hat{\theta}_{u_0}), \nabla^2 L(z, \hat{\theta}_{u_0}) H^{-1} \nabla f_Z(\hat{\theta}_{u_0}) \right\rangle = 0. \end{aligned}$$

Accordingly we have

$$\sum_{y \in Z} \frac{\partial^2}{\partial \epsilon_y \partial \epsilon_z} L(z', \hat{\theta}_{u_0}) = n \frac{\partial}{\partial \epsilon_z} L(z', \hat{\theta}_{u_0}),$$

and Lemma 6 follows.  $\square$

*Proof of Lemma 7.* To establish eq. (11), instead of summing over all  $y \in Z$ , we introduce the term  $O(n^{-2})$  and single out the two terms  $y = z$  and  $y = z'$

$$\sum_{y \neq z, z'} \left[ \frac{\partial^2}{\partial \epsilon_y \partial \epsilon_z} L(z', \hat{\theta}_{u_0}) \frac{1}{n} + O(n^{-2}) \right] + \left[ \frac{\partial^2}{\partial \epsilon_{z'} \partial \epsilon_z} L(z', \hat{\theta}_{u_0}) + \frac{\partial^2}{\partial \epsilon_z \partial \epsilon_z} L(z', \hat{\theta}_{u_0}) \right] \frac{1}{n} + O(n^{-2}) = \langle \nabla L(z', \hat{\theta}), \nabla L(z, \hat{\theta}_{u_0}) \rangle + O(n^{-1}),$$

since  $\sum_{y \in Z} O(n^{-2}) = O(n^{-1})$ . We immediately observe

$$\left[ \frac{\partial^2}{\partial \epsilon_{z'} \partial \epsilon_z} L(z', \hat{\theta}_{u_0}) + \frac{\partial^2}{\partial \epsilon_z \partial \epsilon_z} L(z', \hat{\theta}_{u_0}) \right] \frac{1}{n} + O(n^{-2}) = O(n^{-1}),$$

and arrive at

$$\begin{aligned} \sum_{y \neq z, z'} \left[ \frac{\partial^2}{\partial \epsilon_y \partial \epsilon_z} L(z', \hat{\theta}_{u_0}) \frac{1}{n} + O(n^{-2}) \right] &= \langle \nabla L(z', \hat{\theta}_{u_0}), \nabla L(z, \hat{\theta}_{u_0}) \rangle + O(n^{-1}) \\ &= \frac{\partial}{\partial \epsilon_z} L(z', \hat{\theta}_{u_0}) + O(n^{-1}), \end{aligned}$$

whence Lemma 7.  $\square$

*Proof of Theorem 1.* We view  $\left[ \frac{\partial}{\partial \epsilon_z} L(z', \hat{\theta}_u) \right]^k$  as a function of  $\epsilon = (\epsilon_t)_t$ , form its Taylor expansion at  $(\epsilon_t)_t = 0$ , and subsequently evaluate at  $\epsilon = \eta_M$ . This expansion involves terms of partial derivatives  $\frac{\partial}{\partial y}$  for  $y \in M$  and  $s \leq n_0$  guarantess that the number of these terms does not scale with  $n$ . Consequently we obtain

$$(18) \quad \left[ \frac{\partial}{\partial \epsilon_z} L(z', \hat{\theta}_{u_{\eta_M}}) \right]^k - \left[ \frac{\partial}{\partial \epsilon_z} L(z', \hat{\theta}_{u_0}) \right]^k = \sum_{y \in M} \left[ \frac{\partial}{\partial \epsilon_y} \left[ \frac{\partial}{\partial \epsilon_z} L(z', \hat{\theta}_{u_0}) \right]^k \cdot \left( -\frac{1}{n} \right) + O(n^{-2}) \right]$$

Here  $z', z$  are selected as distinct elements of  $Z$  and  $M \subset Z \setminus \{z', z\}$  and the error term  $O(n^{-2})$  is welldefined, since  $s \leq n_0$  and  $n$  is sufficiently large. We next consider pairs  $(M, \{z', z\})$  where  $z, z' \notin M$ . A fixed  $\{z', z\}$  appears in such pairs with multiplicity  $\binom{n-2}{s}$ . Consequently summing over all pairs  $(M, \{z', z\})$  and normalizing by  $\rho_s = \frac{1}{\binom{n}{2} \binom{n-2}{s}}$  we derive

$$\frac{1}{\binom{n-2}{s}} \frac{1}{\binom{n}{2}} \sum_{\substack{(M, \{z', z\}) \\ |M|=s}} \left[ \frac{\partial}{\partial \epsilon_z} L(z', \hat{\theta}_{u_0}) \right]^k = \mathbb{E}[X_{u_0}^k].$$

Note that  $\binom{n}{2} \binom{n-2}{s} = \binom{n-s}{2} \binom{n}{s}$ , where for fixed  $M$ , the coefficient  $\binom{n-s}{2}$  counts how many pairs  $\{z, z'\}$  not contained in  $M$  can be selected. Therefore we can conclude

$$\frac{1}{\binom{n-s}{2}} \sum_{\{z, z'\} \cap M = \emptyset} \left[ \frac{\partial}{\partial \epsilon_z} L(z', \hat{\theta}_{u_{\eta_M}}) \right]^k = \mathbb{E}[X_{u_{\eta_M}}^k],$$

with associated loss function  $f_{Z \setminus M}(\theta) = \frac{1}{n-s} \sum_{t \in Z \setminus M} L(t, \theta)$ , and

$$\begin{aligned} \frac{1}{\binom{n}{s}} \frac{1}{\binom{n-s}{2}} \sum_{\substack{(M, \{z', z\}) \\ |M|=s}} \left[ \frac{\partial}{\partial \epsilon_z} L(z', \hat{\theta}_{u_{\eta_M}}) \right]^k &= \frac{1}{\binom{n}{s}} \sum_{\substack{MCZ \\ |M|=s}} \left[ \frac{1}{\binom{n-s}{2}} \sum_{\{z, z'\} \cap M = \emptyset} \left[ \frac{\partial}{\partial \epsilon_z} L(z', \hat{\theta}_{u_{\eta_M}}) \right]^k \right] \\ &= \frac{1}{\binom{n}{s}} \sum_{\substack{MCZ \\ |M|=s}} \mathbb{E}[X_{u_{\eta_M}}^k]. \end{aligned}$$

Since  $f_{Z \setminus M}$  assumes a minimum at  $\hat{\theta}_{u_{\eta_M}}$  we derive from (18)

$$\begin{aligned} \Delta_s(\mathbb{E}[X_{u_0}^k]) &= \rho_s \sum_{(M, \{z', z\})} \left[ \frac{\partial}{\partial \epsilon_z} L(z', \hat{\theta}_{u_0}) \right]^k - \left[ \frac{\partial}{\partial \epsilon_z} L(z', \hat{\theta}_{u_{\eta_M}}) \right]^k \\ &= \rho_s \sum_{(M, \{z', z\})} \left[ \sum_{y \in M} \left[ \frac{\partial}{\partial \epsilon_y} \left[ \frac{\partial}{\partial \epsilon_z} L(z', \hat{\theta}_{u_0}) \right]^k \right] \cdot \left( \frac{1}{n} \right) + O(n^{-2}) \right] \\ &= k \rho_s \sum_{(M, \{z', z\})} \left[ \left[ \frac{\partial}{\partial \epsilon_z} L(z', \hat{\theta}_{u_0}) \right]^{k-1} \sum_{y \in M} \left[ \frac{\partial^2}{\partial \epsilon_y \partial \epsilon_z} L(z', \hat{\theta}_{u_0}) \cdot \left( \frac{1}{n} \right) + O(n^{-2}) \right] \right] \\ &= k \rho_s \sum_{\{z, z'\}} \left[ \left[ \frac{\partial}{\partial \epsilon_z} L(z', \hat{\theta}_{u_0}) \right]^{k-1} \left[ \sum_M \sum_{y \in M} \left[ \frac{\partial^2}{\partial \epsilon_y \partial \epsilon_z} L(z', \hat{\theta}_{u_0}) \cdot \left( \frac{1}{n} \right) + O(n^{-2}) \right] \right] \right]. \end{aligned}$$

Any given  $y \in Z \setminus \{z, z'\}$  appears in pairs  $(M, \{z, z'\})$  with multiplicity  $\binom{n-3}{s-1}$  and consequently

$$(19) \quad \sum_M \sum_{y \in M} \left[ \frac{\partial^2}{\partial \epsilon_y \partial \epsilon_z} L(z', \hat{\theta}_{u_0}) \cdot \left( \frac{1}{n} \right) + O(n^{-2}) \right] = \binom{n-3}{s-1} \sum_{\substack{y \in Z \\ y \neq z, z'}} \left[ \frac{\partial^2}{\partial \epsilon_y \partial \epsilon_z} L(z', \hat{\theta}_{u_0}) \cdot \left( \frac{1}{n} \right) + O(n^{-2}) \right]$$

Lemma 7 allows us to conclude

$$\begin{aligned} k \rho_s \sum_{\substack{\{z, z'\}, z \neq z' \\ z, z' \in Z}} \left[ \left[ \frac{\partial}{\partial \epsilon_z} L(z', \hat{\theta}_{u_0}) \right]^{k-1} \left[ \binom{n-3}{s-1} \sum_{y \in Z \setminus \{z, z'\}} \left[ \frac{\partial^2}{\partial \epsilon_y \partial \epsilon_z} L(z', \hat{\theta}_{u_0}) \cdot \left( \frac{1}{n} \right) + O(n^{-2}) \right] \right] \right] \\ &= k \rho_s \sum_{\substack{\{z, z'\}, z \neq z' \\ z, z' \in Z}} \left[ \left[ \frac{\partial}{\partial \epsilon_z} L(z', \hat{\theta}_{u_0}) \right]^{k-1} \left[ \binom{n-3}{s-1} \left[ \frac{\partial}{\partial \epsilon_z} L(z', \hat{\theta}_{u_0}) + O(n^{-1}) \right] \right] \right] \\ &= k \frac{\binom{n-3}{s-1}}{\binom{n}{2} \binom{n-2}{s}} \sum_{\substack{\{z, z'\}, z \neq z' \\ z, z' \in Z}} \left[ \left[ \frac{\partial}{\partial \epsilon_z} L(z', \hat{\theta}_{u_0}) \right]^k + O(n^{-1}) \right]. \end{aligned}$$

Since  $\frac{\binom{n-3}{s-1}}{\binom{n-2}{s}} = \frac{s}{n-2}$ ,  $\rho_s^{-1} = \binom{n}{2} \binom{n-2}{s}$ , and

$$\frac{1}{\binom{n}{2}} \sum_{\substack{\{z, z'\}, z \neq z' \\ z, z' \in Z}} \left[ \frac{\partial}{\partial \epsilon_z} L(z', \hat{\theta}_{u_0}) \right]^k = \mathbb{E}[X_{u_0}^k],$$

we arrive at

$$\Delta_s(\mathbb{E}[X_{u_0}^k] = \mathbb{E}[X_{u_0}^k] - \frac{1}{\binom{n}{s}} \sum_{\substack{M \subset Z \\ |M|=s}} \mathbb{E}[X_{u_{\eta M}}^k] = \frac{ks}{n-2} \mathbb{E}[X_{u_0}^k] + \frac{ks}{n-2} O(n^{-1+2-2}),$$

completing the proof of the theorem.  $\square$

*Proof of Theorem 2.* We denote  $X = X_{u_0}$  and  $X_M = X_{u_{\eta M}}$  and compute using Theorem 1 for  $k = 2$

$$\begin{aligned} \mathbb{V}[X] - \frac{1}{\binom{n}{s}} \sum_{\substack{M \subset Z \\ |M|=s}} \mathbb{V}[X_M] &= [\mathbb{E}[X^2] - \mathbb{E}[X]^2] - \frac{1}{\binom{n}{s}} \sum_{\substack{M \subset Z \\ |M|=s}} [\mathbb{E}[X_M^2] - \mathbb{E}[X_M]^2] \\ &= \left[ \mathbb{E}[X^2] - \frac{1}{\binom{n}{s}} \sum_{\substack{M \subset Z \\ |M|=s}} \mathbb{E}[X_M^2] \right] - \left[ \mathbb{E}[X]^2 - \frac{1}{\binom{n}{s}} \sum_{\substack{M \subset Z \\ |M|=s}} \mathbb{E}[X_M]^2 \right] \\ &= \left[ \frac{2s}{n-2} \mathbb{E}[X^2] + O(n^{-2}) \right] - \left[ \mathbb{E}[X]^2 - \frac{1}{\binom{n}{s}} \sum_{\substack{M \subset Z \\ |M|=s}} \mathbb{E}[X_M]^2 \right] \end{aligned}$$

It remains to compute the second term: we claim that for any  $M$  holds  $\mathbb{E}[X_M] = \mathbb{E}[X] = O(n^{-1})$ . This follows from  $\nabla f_Z(\hat{\theta}_{u_0}) = \nabla f_{Z \setminus M}(\hat{\theta}_{u_{\eta M}}) = 0$ , and Lemma 3. For  $\hat{\theta} = \hat{\theta}_{u_{\eta M}}$ ,  $|M| = s$  we have

$$\sum_{z, z' \in Z \setminus M} \frac{\partial}{\partial \epsilon_z} L(z', \hat{\theta}) = \sum_{z' \in Z \setminus M} \nabla L(z', \hat{\theta})^T H^{-1} \left( \sum_{z \in Z \setminus M} \nabla L(z, \hat{\theta}) \right) = 0.$$

and setting  $M = \emptyset$ ,  $s = 0$  we obtain an analogous expression for  $X_{u_0}$ . This in turn implies  $\mathbb{E}[X_{u_0}] = \mathbb{E}[X_{u_{\eta M}}] = O(n^{-1})$  and consequently,

$$\mathbb{E}[X]^2 - \frac{1}{\binom{n}{s}} \sum_{\substack{M \subset Z \\ |M|=s}} \mathbb{E}[X_M]^2 = O(n^{-2}),$$

establishing

$$\begin{aligned} \mathbb{V}[X] - \frac{1}{\binom{n}{s}} \sum_{\substack{M \subset Z \\ |M|=s}} \mathbb{V}[X_M] &= \left[ \frac{2s}{n-2} \mathbb{E}[X^2] + O(n^{-2}) \right] + O(n^{-2}) \\ &= \frac{2s}{n-2} (\mathbb{E}[X^2] - \mathbb{E}[X]^2) + O(n^{-2}). \end{aligned}$$

$\square$

*Proof of Corollary 1.* We prove the corollary by contradiction, suppose (13) does not hold. Then for any  $M \subset Z$  with  $|M| = s$  holds

$$\frac{2s}{n-2} \mathbb{E}[X_{u_0}^k] + O(n^{-2}) > \mathbb{E}[X_{u_0}^k] - \mathbb{E}[X_{u_{\eta M}}^k].$$

Summing over all such  $M \subset Z$  and normalizing by  $\frac{1}{\binom{n}{s}}$  has no effect on any terms that are independent of  $M$ , whence we arrive at

$$\frac{2s}{n-2} \mathbb{E}[X_{u_0}^k] + O(n^{-2}) > \mathbb{E}[X_{u_0}^k] - \frac{1}{\binom{n}{s}} \sum_{\substack{Z \subset M \\ |Z|=s}} \mathbb{E}[X_{u_{nM}}^k]$$

which is in view of Theorem 1, impossible.  $\square$

#### DATA SETS AND SOURCE CODE

The source code used for the experiments in this paper is available as part of the Git repository:

<https://github.com/FenixHuang667/DataPurification>

Python v.3.12.3 was used with PyTorch v.2.9.0. The data displayed in Figures 3–8 through Section 4 is included in the Git repository.

#### ACKNOWLEDGEMENTS

Funding provided by the UVA National Security & Data Institute, Contracting Activity # 2024-24070100001. We thank Phillip Potter for discussions and feedback on the manuscript, we gratefully acknowledge the help of Jingyi Gao for preparing the EMNIST data.

#### REFERENCES

- [1] Zeyuan Allen-Zhu, Yuanzhi Li, and Zhao Song. A convergence theory for deep learning via overparameterization. In Kamalika Chaudhuri and Ruslan Salakhutdinov, editors, *Proceedings of the 36th International Conference on Machine Learning*, volume 97 of *Proceedings of Machine Learning Research*, pages 242–252. PMLR, 09–15 Jun 2019.
- [2] Tara Baldacchino, Elizabeth J. Cross, Keith Worden, and Jennifer Rowson. Variational Bayesian mixture of experts models and sensitivity analysis for nonlinear dynamical systems. *Mechanical Systems and Signal Processing*, 66–67:178–200, 2016.
- [3] Christopher Barrett, Andrei Bura, Fenix Huang, and Christian Reidys. Towards an information-theoretic framework for multiple sequence alignment sub-sampling. *Proceedings of the Royal Society A: Mathematical, Physical and Engineering Sciences*, 480(2304):20230797, 12 2024.
- [4] Samyadeep Basu, Philip Pope, and Soheil Feizi. Influence functions in deep learning are fragile. *arXiv preprint arXiv:2006.14651*, 2020.
- [5] Zixiang Chen, Yihe Deng, Yue Wu, Quanquan Gu, and Yuanzhi Li. Towards understanding the mixture-of-experts layer in deep learning. In S. Koyejo, S. Mohamed, A. Agarwal, D. Belgrave, K. Cho, and A. Oh, editors, *Advances in Neural Information Processing Systems*, volume 35, pages 23049–23062. Curran Associates, Inc., 2022.
- [6] Gregory Cohen, Saeed Afshar, Jonathan Tapson, and Andre van Schaik. EMNIST: Extending MNIST to handwritten letters. In *2017 International Joint Conference on Neural Networks (IJCNN)*, pages 2921–2926. IEEE, 2017.
- [7] R. Dennis Cook and Sanford Weisberg. Characterizations of an empirical influence function for detecting influential cases in regression. *Technometrics*, 22(4):495–508, 1980.
- [8] David Eigen, Marc’Aurelio Ranzato, and Ilya Sutskever. Learning factored representations in a deep mixture of experts, 2014. version 3.
- [9] Jacob R Epifano, Ravi P Ramachandran, Aaron J Masino, and Ghulam Rasool. Revisiting the fragility of influence functions. *Neural Networks*, 162:581–588, 2023.
- [10] Borjan Geshkovski, Cyril Letrouit, Yury Polyanskiy, and Philippe Rigollet. A mathematical perspective on transformers html articles powered by ams mathviewer. *Bull. Amer. Math. Soc.*, 62:427–479, 2025.
- [11] Zayd Hammoudeh and Daniel Lowd. Training data influence analysis and estimation: A survey. *Machine Learning*, 113(5):2351–2403, 2024.

- [12] Frank R. Hampel, Elvezio M. Ronchetti, Peter J. Rousseeuw, and Walter A. Stahel. *Robust Statistics: The Approach Based on Influence Functions*. Wiley, 1986.
- [13] Christian Hennig. *Identifiability of Finite Linear Regression Mixtures*. Universität Hamburg. Institut für Mathematische Stochastik, 1996.
- [14] Robert A. Jacobs, Michael I. Jordan, Steven J. Nowlan, and Geoffrey E. Hinton. Adaptive mixtures of local experts. *Neural Computation*, 3(1):79–87, 1991.
- [15] Diederik P. Kingma and Max Welling. Auto-encoding variational bayes. *arXiv preprint arXiv:1312.6114*, 2013.
- [16] Pang Wei Koh and Percy Liang. Understanding black-box predictions via influence functions. In Doina Precup and Yee Whye Teh, editors, *Proceedings of the 34th International Conference on Machine Learning*, volume 70 of *Proceedings of Machine Learning Research*, pages 1885–1894. PMLR, 06–11 Aug 2017.
- [17] Frantzeska Lavda, Magda Gregorová, and Alexandros Kalousis. Data-dependent conditional priors for unsupervised learning of multimodal data. *Entropy*, 22(8), 2020.
- [18] Y. LeCun, Y. Bengio, and G. Hinton. Deep learning. *Nature*, 521:436–444, 2015.
- [19] Zhe Li, Wei Zhao, Yige Li, and Jun Sun. Do influence functions work on large language models? *arXiv preprint arXiv:2409.19998*, 2024.
- [20] Tianyang Lin, Yuxin Wang, Xiangyang Liu, and Qiu. Xipeng. A survey of transformers. *AI Open*, 3:111–132, 2022.
- [21] Fred L Mannerling, Venky Shankar, and Chandra R Bhat. Unobserved heterogeneity and the statistical analysis of highway accident data. *Analytic methods in accident research*, 11:1–16, 2016.
- [22] Siyuan Mu and Sen Lin. A comprehensive survey of mixture-of-experts: Algorithms, theory, and applications, 2025.
- [23] Samyajoy Pal and Christian Heumann. Flexible multivariate mixture models: A comprehensive approach for modeling mixtures of non-identical distributions. *International Statistical Review*, 2024.
- [24] Adam Paszke, Sam Gross, Francisco Massa, Adam Lerer, James Bradbury, Gregory Chanan, Trevor Killeen, Zeming Lin, Natalia Gimelshein, Luca Antiga, Alban Desmaison, Andreas Köpf, Edward Yang, Zach DeVito, Martin Raison, Alykhan Tejani, Sasank Chilamkurthy, Benoit Steiner, Lu Fang, Junjie Bai, and Soumith Chintala. PyTorch: an imperative style, high-performance deep learning library. In *Proceedings of the 33rd International Conference on Neural Information Processing Systems*, Red Hook, NY, USA, 2019. Curran Associates Inc.
- [25] Noam Shazeer, Azalia Mirhoseini, Krzysztof Maziarz, Andy Davis, Quoc Le, Geoffrey Hinton, and Jeff Dean. Outrageously large neural networks: The sparsely-gated mixture-of-experts layer. In *5th International Conference on Learning Representations (ICRL 2017)*, pages 878–896, 2017.
- [26] Aman Singh and Tokunbo Ogunfunmi. An overview of variational autoencoders for source separation, finance, and bio-signal applications. *Entropy*, 24(1), 2022.
- [27] Harsh Vardhan, Avishek Ghosh, and Arya Mazumdar. Learning and generalization with mixture data. *arXiv preprint arXiv:2504.20651*, 2025.
- [28] Ashish Vaswani, Noam Shazeer, Niki Parmar, Jakob Uszkoreit, Llion Jones, Aidan N Gomez, Łukasz Kaiser, and Illia Polosukhin. Attention is all you need. In *Advances in Neural Information Processing Systems*, pages 5998–6008, 2017.

BIOCOMPLEXITY INSTITUTE, UNIVERSITY OF VIRGINIA

*Email address:* fwh3zc@virginia.edu

DEPARTMENT OF SYSTEMS AND INFORMATION ENGINEERING, UNIVERSITY OF VIRGINIA

*Email address:* henning.mortveit@virginia.edu

DEPARTMENT OF MATHEMATICS, UNIVERSITY OF VIRGINIA

*Email address:* cmr3hk@virginia.edu